Spectrochimica Acta Part A: Molecular and Biomolecular Spectroscopy 138 (2015) 517–528

Contents lists available at ScienceDirect

Spectrochimica Acta Part A: Molecular and Biomolecular Spectroscopy

journal homepage: www.elsevier.com/locate/saa

Nano structure zinc (II) Schiff base complexes of a N_3-tridentate ligand as new biological active agents: Spectral, thermal behaviors and crystal structure of zinc azide complex

M. Montazerozohori [a,*], S. Mojahedi Jahromi [a], A. Masoudiasl [a], P. McArdle [b]

[a] Department of Chemistry, Yasouj University, Yasouj 75918-74831, Iran
[b] School of Chemistry, National University of Ireland, Galway, Ireland

HIGHLIGHTS

- A new series of five coordinated zinc halide complexes of a N_3-tridentate Schiff base is presented.
- The nano-structure zinc complexes were prepared.
- Zinc azide complex structure was analyzed by X-ray crystallography.
- All compounds were tested for their *in vitro* antimicrobial activities.
- Thermal behaviors of all complexes were investigated by thermal analyses.

GRAPHICAL ABSTRACT

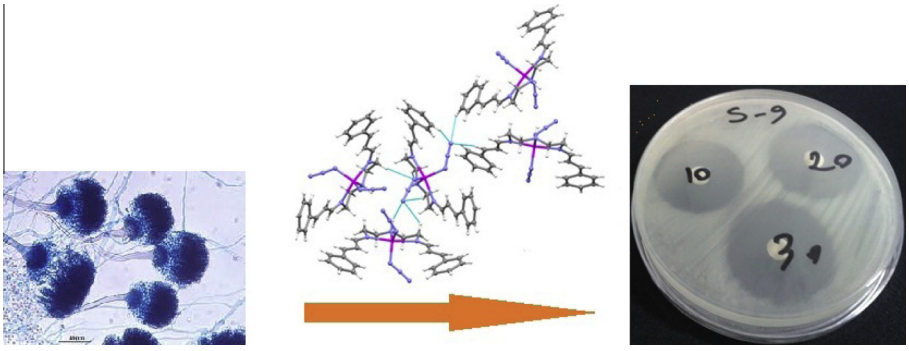

ARTICLE INFO

Article history:
Received 7 September 2014
Received in revised form 19 October 2014
Accepted 20 November 2014
Available online 28 November 2014

Keywords:
Zinc (II)
Tridentate
Nano-structure
X-ray
Biological
Thermal

ABSTRACT

In this work, synthesis of some new five coordinated zinc halide/pseudo-halide complexes of a N_3-tridentate ligand is presented. All complexes were subjected to spectroscopic and physical methods such as FT-IR, UV–visible, ^{1}H and ^{13}C NMR spectra, thermal analyses and conductivity measurements for identification. Based on spectral data, the general formula of $ZnLX_2$ (X = Cl^-, Br^-, I^-, SCN^- and N_3^-) was proposed for the zinc complexes. Zinc complexes have been also prepared in nano-structure sizes under ultrasonic irradiation. X-ray powder diffraction (XRD), scanning electron microscopy (SEM) and transmission electron microscopy (TEM) were applied for confirmation of nano-structure character for the complexes. Among the complexes, zinc azide complex structure was analyzed by X-ray crystallography. This complex crystallizes as a triplet in trigonal system with space group of $P3_1$. The coordination sphere around the zinc center is well shown as a distorted trigonal bipyramidal with three nitrogen atoms from Schiff base ligand and two terminal azide nitrogen atoms attached to zinc ion. Various intermolecular interactions such as N—H···N, C—H···N and C—H···π hydrogen bonding interactions stabilize crystalline lattice so that they causes a three dimensional supramolecular structure for the complex. *In vitro* screening of the compounds for their antimicrobial activities showed that $ZnLI_2$, $ZnL(N_3)_2$, $ZnLCl_2$ and $ZnL(NCS)_2$ were found as the most effective compound against bacteria of *Bacillus subtilis*, *Staphylococcus aureus*, *Pseudomonas aeruginosa* and *Escherichia coli* respectively. Also $ZnLI_2$ and $ZnLCl_2$ complexes were found more effective against two selected fungi than others. Finally, thermal behaviors of the zinc complexes showed that they are decomposed via 2–4 thermal steps from room temperature up to 1000 °C.

* Corresponding author. Tel./fax: +98 74133223048.
E-mail address: mmzohory@yahoo.com (M. Montazerozohori).

http://dx.doi.org/10.1016/j.saa.2014.11.055
1386-1425/

Introduction

Bioinorganic chemistry is an active research area for inorganic chemists that it has been initiated from the successive synthesis of *cis*-platin as an anticancer drug [1,2]. As found in many reports, metal ions have enhanced the efficacy of organic drugs when the metals placed in their structures [3,4]. Metal coordination compounds have a constructive role in biological activity point of view [5–9]. Among various complexes, Schiff base metal complexes are more pleasant than many other ones [10]. They are easily synthesized and have excellent characteristics and applications in various scientific fields such as biochemistry, optical, catalysis, agriculture, dye and enzyme modeling [11–13]. A literature survey shows notable biological activities of the Schiff base metal complexes including antibacterial, antifungal, anti-flammatory, analgesic, anti-tubercular, anti-oxidant activities and antiviral effects [14–20]. In addition, possibility of ligand exchange in Schiff base complexes provides an opportunity to design and synthesize of new product for especial biological usage with regard to bacterial resistant to current organic-based drugs. The interaction of these complexes with DNA leading to binding or cleavage proposes their anti-cancer potentials as new therapeutic agents [21–23]. These useful utilities cause the Schiff bases play an important role in medicinal chemistry field and are considered as target substance for many synthetic scientists. The study of nano structure compounds is an extremely popular field because of their unique properties that are absolutely different with respect to them in bulk phase that is related to the large numbers of surface molecules. Choosing the proper synthetic process is an important factor in control of the size of materials at the sub micrometer scale so that selecting a proper method is a serious step in nanotechnology field [24,25]. Nano structure inorganic zinc compounds have been reported [26,27] but the reports for nano structure coordination zinc compound are rarely found.

Herein, in continuation of our previous reports [28–33] the synthesis and characterization of some new zinc complexes of a tridentate Schiff base ligand entitled as (E)-N1-((E)-3-phenylallylidene)-N2-(2-((E)-((E)-3-phenylallylidene) amino) ethyl) ethane-1,2-diamine are presented. The nano-structure zinc complexes were also prepared under ultrasonic irradiation. Zinc azide complex structure was analyzed by X-ray crystallography. Furthermore, antibacterial/antifungal properties and thermal behaviors (TG/DTG/DTA) of all zinc complexes are investigated.

Experimental

Materials and methods

All chemicals such as trans-3-phenyl-2 propenal, diethylenetriamine and zinc salts were provided from the Aldrich and/or Merck chemical companies in high purity. Zinc thiocyanate and azides were freshly prepared according to our previous report [28]. Infrared spectra were obtained by a JASCO-FT/IR680 instrument on the range of 4000–400 cm^{-1} as KBr pellets. A Bruker DPX FT/NMR-400 spectrometer was applied to record ^1H and ^{13}C NMR spectra in dimethylsulfoxide. The electronic spectra of the compounds in chloroform were obtained from a JASCO-V570 spectrophotometer instrument in the range of 200–800 nm. BUCHI B-545 instrument was applied for recording of melting points or decomposition temperature of the complexes. A Metrohm-712 conductometer with a dip-type conductivity cell made of platinum black was applied for measurements of molar conductivities of the compound in chloroform and/or dimethylformamide. A Perkin–Elmer Pyris model instrument was applied for record of thermo-gravimetric diagrams. Scanning electron microscopy (SEM) images were captured on a Hitachi S-1460 field emission scanning electron microscope using Ac voltage of 15 kV. TEM image was obtained on instruments of Philips CM-10 TEM microscope operated at 100 kV. X-ray powder diffraction (XRD) spectra were recorded on a STOE type STIDY-MP-Germany X-ray diffractometer with Cu Kα radiation (λ = 1.5418). The high-power ultrasonic unit Bandelin Super Sonorex RK-100H with ultrasonic peak output 320 W and HF power 80 Weff has been used for preparation of nano structure complexes.

Synthesis of ligand

The ligand was synthesized according to previous report via a condensation reaction between trans-3-phenyl-2 propenal, and diethylenetriamine in 2:1 M ratio in ethanol solvent under vigorous stirring at room temperature [33].

Synthesis of zinc complexes

For the synthesis of the zinc complexes, the fresh ligand solution was gradually added to zinc halide, thiocyanate or azide salts solution as equimolar in ethanol under severe stirring and then the mixture was stirred about 1–2 h at room temperature. At the end, the obtained precipitate of zinc complexes was filtered and washed with ethanol. For more purification, the products were recrystallized from dichloromethane/ethanol mixture (1:1) and then dried in vacuum. The physical and spectral data (IR and UV–visible) of the compounds have been compiled in Tables 1 and 2. The ^1H and ^{13}C NMR data of zinc complexes based on Scheme 1 are listed as follow:

Ligand(L); ^{1}HNMR(in DMSO): 7.79(d, 1H$_f$, J = 10.02 Hz), 7.76(dd, 2H$_c$, J = 6.80 Hz, J = 3.30 Hz), 7.61(bd, 2H$_{c'}$, J = 7.49 Hz), 7.48(m, 7H$_{bb',aa',e'}$), 7.11(d, 1H$_d$, J = 16.22 Hz), 7.00(d, 1H$_{d'}$, J = 16.21 Hz), 6.87(dd, 1H$_e$, J = 15.96 Hz, J = 7.59 Hz), 4.05(m, 1H$_f$), 3.98(m, 2H$_{g'}$), 3.89(m, 2H$_{h'}$), 3.82(m, 2H$_h$), 3.74(bs, 2H$_g$), 3.19(bs, 1H$_{NH}$). ^{13}CNMR (in DMSO): ^{13}C NMR (in DMSO): 167.02(C$_7$), 146.79(C$_{5,5'}$), 131.22(C$_{4,4'}$), 129.07(C$_{1,1'}$), 128.72(C$_{2,2}$), 128.49(C$_{3,3'}$), 127.47(C$_{6,6'}$), 108.37(C$_{7'}$) 55.52(C$_{9'}$), 49.87(C$_9$), 43.63(C$_8$), 42.37(C$_{8'}$) ppm [33].

[ZnLCl$_2$]: ^{1}HNMR (in DMSO): 8.26 (d, 2H$_{ff'}$, J = 8.99 Hz), 7.78(m, 2H$_{ee'}$), 7.60(d, 4H$_{cc'}$, J = 6.98 Hz), 7.47(m, 6H$_{bb',aa'}$), 7.25(d, 2H$_{dd'}$, J = 15.67 Hz), 3.66(bs, 4H$_{hh'}$), 2.90(bs, 4H$_{gg'}$ and 1H$_{NH}$) ppm. ^{13}CNMR (in DMSO): 166.07(C$_{7,7'}$), 143.81(C$_{5,5'}$), 135.36 (C$_{4,4'}$), 129.78(C$_{1,1'}$), 129.04(C$_{2,2'}$), 128.66(C$_{3,3'}$), 127.45(C$_{6,6'}$), 56.02(C$_{8,8'}$), 48.14(C$_{9,9'}$) ppm.

[ZnLBr$_2$]: ^{1}HNMR (in DMSO): 8.31(d, 2H$_{ff'}$, J = 8.99 Hz), 7.80 (dd, 2H$_{ee'}$, J = 15.80 Hz, J = 8.40 Hz), 7.62(d, 4H$_{cc'}$, J = 7.19 Hz), 7.47 (m, 6H$_{bb,\ aa'}$) 7.27(d, 2H$_{dd'}$, J = 16.00 Hz), 3.68(m, 4H$_{hh'}$), 2.93(bs, 4H$_{gg'}$ and 1H$_{NH}$) ppm. ^{13}CNMR (in DMSO): 166.46(C$_{7,7'}$), 144.31(C$_{5,5'}$), 135.30 (C$_{4,4'}$), 129.92(C$_{1,1'}$), 129.09(C$_{2,2'}$), 127.50 (C$_{3,3'}$), 126.86(C$_{6,6'}$), 55.98(C$_{8,8'}$), 48.14 (C$_{9,9'}$) ppm.

[ZnLI$_2$]: ^{1}HNMR (in DMSO): 8.37(d, 2H$_{ff'}$, J = 8.69 Hz), 7.78(md, 2H$_{ee'}$, J = 25.12 Hz), 7.63(d, 2H$_c$, J = 7.23 Hz), 7.56(d, 2H$_c$, J = 7.45 Hz), 7.47(m, 6H$_{bb',aa'}$), 7.43(d, 2H$_{dd'}$, J = 22.51 Hz), 3.64(bs, 4H$_{hh'}$), 2.95(bs, 4H$_{gg'}$ and 1H$_{NH\ '}$) ppm. ^{13}CNMR (in

Table 1
Analytical and physical data of the zinc complexes.

Run	Complexes	Color	M.P(Dec.[a]) (°C)	Yield (%)	$\Lambda°_M$ ($cm^2\ \Omega^{-1}\ M^{-1}$)
1	$ZnLCl_2$	Cream	150	40	0.018
2	$ZnLBr_2$	Orange	159	65	0.014
3	$ZnLI_2$	Orange	130	70	0.31
4	$ZnL(NCS)_2$	Yellow	208	84	0.019
5	$ZnL(N_3)_2$	Cream	137	40	0.017

[a] (Dec.) refers to decomposition temperature of the compounds.

Table 2
Vibrational (cm^{-1}) and electronic spectral data of tridentate Schiff base (L) and its zinc complexes.

Compound	νCH_{arom}	$\nu N{-}H_{amine}$	νCH (alkene)	νCH (aliph.)	νCH (imine)	$\nu(SCN/N_3)$	νC=N	νC=C	νM–N	λ_{max}(nm) (ε, $cm^{-1}\,M^{-1}$)
Ligand	3056	245	3025	2925	2834	–	1635	1492–1450	–	228(33951)–281(30840) [33]
$ZnLCl_2$	3057	3234	3025	2934	2873	–	1632	1492–1450	506	227(18594)–297(22182)
$ZnLBr_2$	3056	3214	3025	2931	2876	–	1630	1490–1450	505	227(20521)–298(27665)
$ZnLI_2$	3054	3205	3022	2927	2867	–	1630	1489–1449	507	227(23880)–299(32862)
$ZnL(NCS)_2$	3056	3211	3023	2929	2880	2075	1633	1488–1448	447	226(20938)–297(35292)
$ZnL(N_3)_2$	3054	3210	3026	2927	2877	2063	1632	1488–1469	445	229(19301)–291(31760)

(ε) Refers to absorption coefficient.

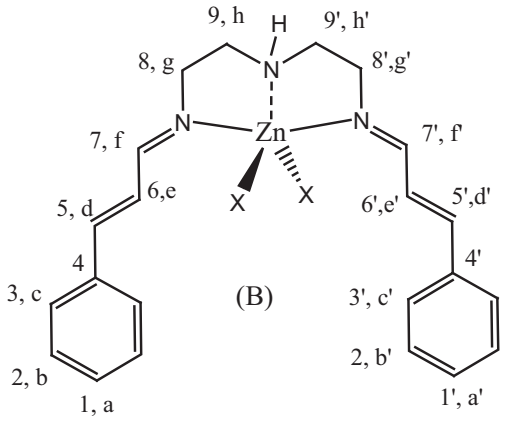

Scheme 1. The structure of the zinc complexes.

DMSO): 167.69($C_{7,7'}$), 146.26($C_{5,5'}$), 134.76($C_{4,4'}$), 130.37($C_{1,1'}$), 129.11($C_{2,2'}$), 127.63 ($C_{3,3'}$), 125.43($C_{6,6'}$), 55.43 ($C_{8,8'}$), 46.49 ($C_{9,9'}$) ppm.
[$ZnL(NCS)_2$]: ^{1}HNMR (in DMSO): 8.36(d, $2H_{f,f'}$, J = 9.20 Hz), 7.78(d, $4H_{c,c'}$, J = 6.75 Hz), 7.51(m, $4H_{ee',a,a'}$), 7.44(t, $4H_{bb'}$, J = 6.34 Hz), 7.38(d, $2H_{dd'}$, J = 15.88 Hz), 3.63(bs, $4H_{h,h'}$), 2.86(bs, $4H_{g,g'}$ and $1H_{NH}$) ppm. ^{13}CNMR (in DMSO): 167.61 ($C_{7,7'}$), 146.26($C_{5,5'}$), 134.89 ($C_{4,4'}$), 134.01(C_{NCS}), 130.19($C_{1,1'}$), 128.97($C_{2,2'}$), 128.01($C_{3,3'}$), 125.12($C_{6,6'}$), 56.11($C_{8,8'}$), 47.26 ($C_{9,9'}$) ppm.
[$ZnL(N_3)_2$]: ^{1}HNMR (in DMSO): 8.37(d, $2H_{ff'}$, J = 8.85 Hz), 7.70(d, $4H_{c,c'}$, J = 6.95 Hz), 7.47(m, $6H_{b,b',a,a'}$), 7.35(d, $2H'_{dd'}$, J = 15.89 Hz), 7.24(dd, $2H'_{ee'}$, J = 15.89 Hz, J = 8.94 Hz), 3.64(bs, $4H_{h,h'}$), 2.88(bs, $4H_{gg'}$ and $1H_{NH}$) ppm. ^{13}CNMR (in DMSO): 166.74($C_{7,7'}$), 145.17 ($C_{5,5'}$), 135.18 ($C_{4,4'}$), 129.96($C_{1,1'}$), 129.03($C_{2,2'}$), 127.77 ($C_{3,3'}$), 126.02($C_{6,6'}$), 55.83($C_{8,8'}$), 48.04 ($C_{9,9'}$) ppm.

Synthesis of nano-structure zinc complexes

An ethanolic solution of the tridentate ligand (1 mmol in 20 mL) was drop wise added into a zinc salts in ethanol (1 mmol in 20 mL) during 30 min under ultrasonic irradiation. After complete addition, the solution was kept in the ultrasonic bath for a period of 60 min. The obtained precipitates were filtered and dried.

Single crystal X-ray diffraction

An Oxford Diffraction Xcalibur system was used to collect X-ray diffraction data at 150 K. The crystal structures were solved by direct methods (Shelxs-97) and refined by full matrix least-squares using Shelxl-2014 within the Oscail package [34,35].

Antibacterial study (in vitro)

Antibacterial properties of the zinc complexes as compared with free ligand were studied *in vitro* against two Gram-negative (*Pseudomonas aeruginosa* (ATCC: 9027) and *Escherichia coli* (ATCC: 25922) and two Gram-positive bacterial strains (*Bacillus subtilis* (ATCC: 6633) and *Staphylococcus aureus* (ATCC: 6538) by the disk diffusion method [36]. All bacteria were inoculated on the surface of the Muller Hinton Agar (Merck) (24 h old), including nearly 0.5×10^6 colony forming units (CFU/mL), and then were spread by a sterile cotton swab. The trial samples were prepared in specific concentrations (10, 20 and 30 mg/mL in DMSO) in the sample tubes. In the disk diffusion method, the sterilized paper disks (6.4 mm in diameter and adsorption capacity of 50 μL) were soaked in the complexes solution and located on the inoculated Muller Hinton Agar medium. After incubation of the plates at 37 °C for 24 h, the antibacterial activities were evaluated by measuring the diameter of inhibition zone (in mm) of the growth around the disks on the plates. Amoxicillin, Penicillin and Cephalexin were selected as reference bactericidal drugs (positive controls) for any comparison in our conditions. A blank test showed no effect for DMSO against microorganisms studied in this work [30,37].

Antifungal study (in vitro)

Candida albicans and *Aspergillus niger* were our candidate for *in vitro* investigation of the antifungal activities of compounds by disk diffusion method on the surface of Sabouraud Dextrose Agar (Oxoid, Hampshire, England) inoculated with 10^5 (CFU/mL) spore suspension of fungi. The disks were put at the different positions on the agar surface of plates whereas were impregnated with the compound solutions (10, 20 and 30 mg/mL in DMSO). The Petri dishes of *C. albicans* were incubated at 34 °C for 24–48 h while the Petri dishes of *A. niger* were incubated at 38 °C for 7 days. Finally, diameter of inhibition zones around the disks was measured as antifungal activities of the compounds.

Results and discussion

Physical and analytical data

Based on physical and analytical data presented in table 1, general formula of $ZnLX_2$ (X = Cl^-, Br^-, I^-, SCN^- and N_3^-) is proposed the complexes that has been exhibited in Scheme 1. The X-ray crystallography of $ZnL(N_3)_2$ confirmed the suggested structure for the complexes as shown in Scheme 1. Ligand is obtained as viscose oil but all complexes are formed as solid powders. All compounds are stable at room temperature. Solubility test of the compounds in different solvents indicated that chloroform, dichloromethane, dimethylformamide and dimethylsulfoxide are suitable solvent for them. Melting points or decomposition temperature of the zinc complexes are placed in the range of 129–208 °C as found in Table 1. The molar conductivity values of zinc complexes were evaluated in dichloromethane (10^{-3} M) at room temperature suggesting non-electrolytic nature for them.

XRD analysis

X-ray powder diffraction (XRD) patterns of $ZnLCl_2$, $ZnLBr_2$ and $ZnLI_2$ have been recorded in the 2θ range of 0° to 90° to study

the particle size and size distribution of them. XRD patterns of the zinc complexes show the sharp crystalline peaks indicating their crystalline phase. The XRD patterns of zinc chloride, bromide and iodide complexes have been presented in Fig. 1.

The average particle size of the complexes has been calculated using Sherrer's formula from the broadening of the XRD peaks ($D = 0.891\lambda/\beta \cos\theta$, where D is the average grain size, λ is the X-ray wavelength, θ and β are the diffraction angle and full-width at half maximum of an observed peak, respectively). The average crystallite size of the particles was found to be around 32.2 nm and 27.6 nm for $ZnLCl_2$ and for $ZnLBr_2$ respectively. The size distribution plots of the complexes have been displayed as column plots in Fig. 2.

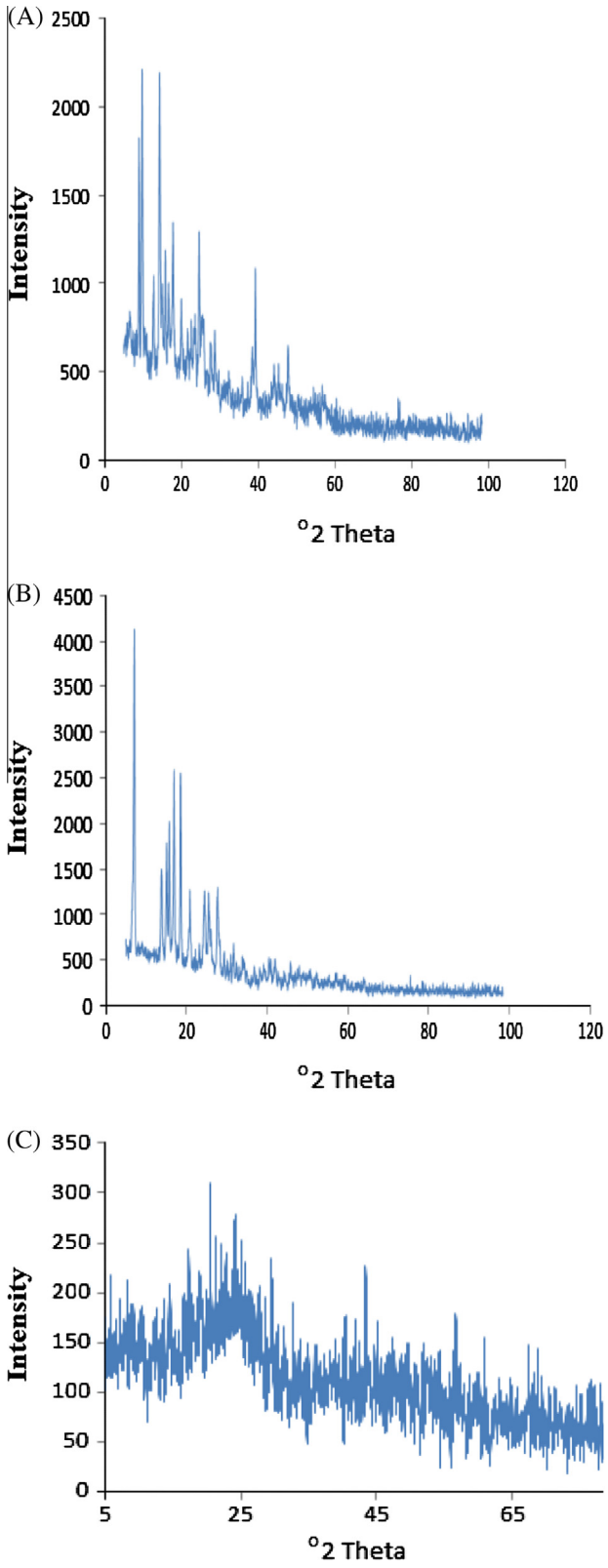

Fig. 1. XRD patterns of zinc chloride (A), bromide (B) and iodide (C) complexes.

SEM and TEM of the compounds

SEM images of zinc complexes were recorded to show the morphologies of nano-structure character of them. From the SEM images (Fig. 3), it is observed that grains are well resolved. Irregularly shaped particles and agglomerated structure are observed so that non-uniform morphology is seen. Also as Fig. 3 represents, the morphologies of nano structure compounds are different for various complexes.

As a typical picture, TEM image of zinc thiocynate complex has been recorded and exhibited in Fig. 4. The TEM image well shows

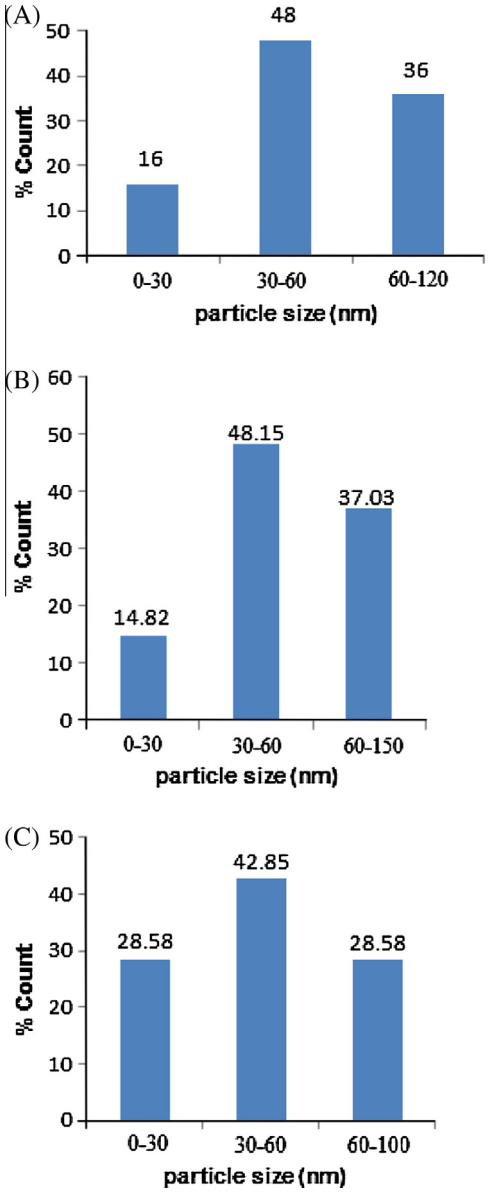

Fig. 2. Particle sizes distribution for nano-structure zinc chloride (A), bromide (B) and iodide (C) complexes.

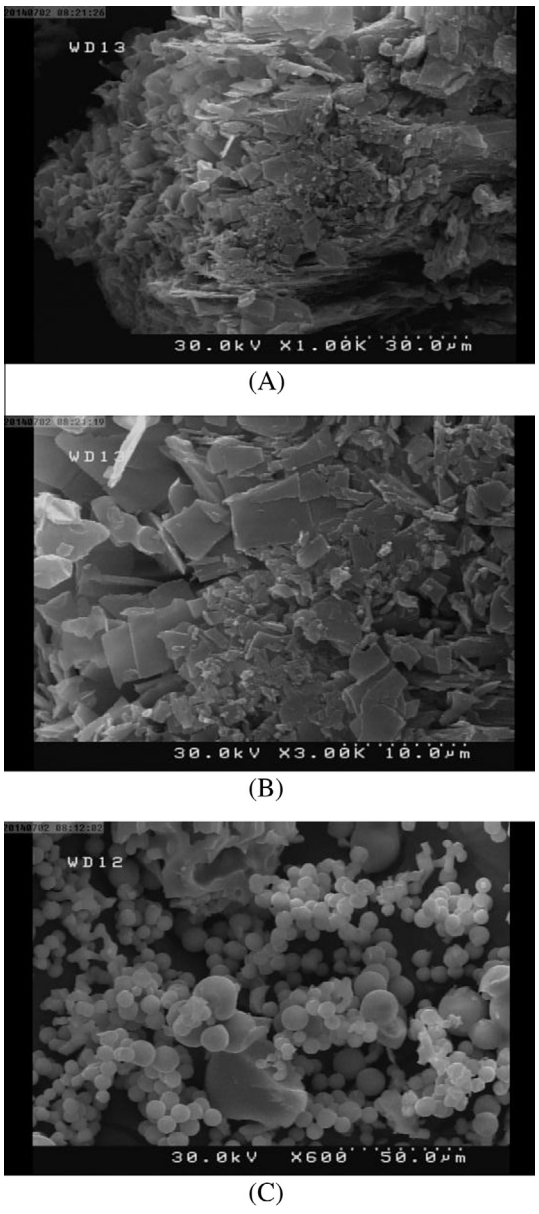

Fig. 3. SEM images of zinc chloride (A), bromide (B) and iodide (C) respectively.

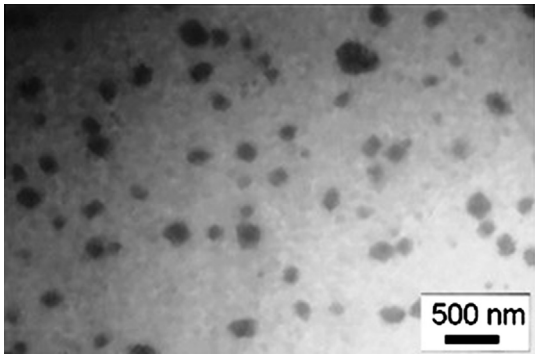

Fig. 4. TEM image of $ZnL(NCS)_2$.

that the average size of zinc thiocynate complex particles is smaller than 100 nm.

These nano-structure Schiff base complexes may show improved properties in current applications of them in analytical, biological and inorganic biochemistry area with respect to bulk analogue.

IR spectral description

Table 2 summarizes vibrational spectral data of the zinc (II) complexes in compared to ligand. Some weak vibrations at 3056, 3025, 2925 and 2834 cm^{-1} in IR spectrum of ligand is found that are attributed to stretching vibrations of aromatic, olefinic, aliphatic and iminic C—H bonds, respectively A broad peak at 3245 cm^{-1} refers to N—H of secondary amine in free ligand. Comparison of the IR data of the zinc complexes with free ligand ones presents good evidences for the coordination of ligand to zinc ion. A meaningful shift of IR spectral data of ligand when it is coordinated to zinc ion is found in Table 2. A sharp band appeared at 1635 cm^{-1} assigned to υ(C=N) (azomethine) of ligand, shifts to lower wave numbers in the range of 1630–1632 cm^{-1} accompanied by an enhancement in intensity in all complexes IR spectra [7,38]. This change well indicates the involvement of azomethine nitrogens in coordination to the zinc center. One reason for the wave number shifts in the complexes spectra, may be due to π-back bonding of metal (d^{10}) to π* of azomethine bond of ligand [39]. Moreover, notable shifts by 11–40 cm^{-1} in vibration of secondary amine group N—H strongly confirms participation of this group in coordination of ligand to zinc ion. In other side, in complexes spectra, some weak absorption frequencies at 445–507 may be due to the stretching vibrations of M–N in the complexes [28–33]. Finally, observation of very strong peaks at 2075 cm^{-1} and 2063 cm^{-1} are considered as powerful evidences supporting the coordination of *N*-thiocyanate and azide anions to zinc ion [40,41].

UV–visible spectra

The electronic spectral data of the ligand and its zinc complexes at concentration of 10^{-5} M in dichloromethane have been tabulated as Table 2. The UV–visible spectrum of the ligand show two considerable absorption bands, one at 227 nm and the other at 281 nm, that may be assigned to π–π* electronic transition of benzene rings and azomethine bonds respectively [29,30]. In the zinc complexes spectra, the first band showed no considerable shift (1–2 nm) whereas the second band appeared as red shifted bands by 9–20 at 290–301 nm that these red shifts is because of elongation in conjugation of system after coordination of the ligand to zinc ion via azomethine nitrogens.

^1H and ^{13}C NMR spectra

The ^1H and ^{13}C NMR spectra of the compounds were recorded in DMSO-d_6 as solvent. Detailed assignments of ^1H and ^{13}C NMR spectra along with coupling constants of the signals for all complexes have been presented in experimental section based on Scheme 1. According to our previous report, the ligand is formed as an imidazolidine Schiff base in one side of structure. After complexation, the ligand ring is opened so a tridentate bis-imine compound is formed based on spectral evidences and X-ray structure. A doublet signal with a coupling constant of 10.02 Hz at 7.79 ppm is assigned to azomethine proton in the ^1H NMR spectrum of ligand. In the complexes spectra, this signal shows downfielded shift to new chemical shifts in the range of 8.26–8.38 Hz that well supports participation of azomethine nitrogen atoms to the zinc ion [42,43]. The aromatic ring protons of the ligand (H_a, $H_{a'}$) and (H_b, $H_{b'}$) appeared as multiple peak at 7.48 ppm. Coordination of ligand to zinc center cause that these signals shift to new position, so we find them as multiplet peaks (may be due to an overlap between ($H_{a,a'}$, $H_{b,b'}$)) in the range of 7.47–7.50 ppm. In an imidazolidine

structure of free ligand [33], H_c and $H_{c'}$ are expected to be different so that they appear at 7.76 and 7.61 ppm as doublet of doublet and broad doublet peaks respectively. In the complexes spectra, H_c and $H_{c'}$ are found as downfielded signals in the range of 7.60–7.78 ppm. In the ^{1}H NMR spectrum of ligand, the signals at 7.11 and 7.00 ppm ppm are attributed to alkenic hydrogens of H_d and $H_{d'}$ respectively. H_d and $H_{d'}$ are observed as a doublet peak with coupling constant of 8.80 Hz as downfielded signal in the range of 7.25–7.44 ppm in the zinc complexes. H_e and $H_{e'}$, after splitting by neighboring hydrogen atoms, appear as multiplet and doublet of doublet signals at 7.48 and 6.87 ppm Hz respectively. After coordination of ligand, these signals notably are downfielded to the range of 7.54–7.97 ppm. In free ligand spectrum, aliphatic hydrogens of $H_{h,h'}$ and $H_{g,g'}$ appear as three multiplet signals and a broad singlet peak in the range of 3.98–3.74 ppm that were downfielded to 3.63–3.3.8 ppm and 2.86–2.95 ppm in zinc complexes respectively. The signal that appears in ligand spectrum at 3.19 ppm may be related to amine proton (NH) that appears in the range of 2.86–2.95 ppm at the zinc complexes spectra. In the ^{13}C NMR spectrum of the ligand, azomethine carbon signal of $C_{(7)}$ appeared at 167.02 ppm. This signal was significantly upfielded to 166.07–166.74 ppm in the zinc complexes that is a powerful evidence to confirm the complex formation via azomethine nitrogen coordination to zinc ion. The signal at 146.79 ppm was attributed to $C_{(5,5')}$ that undergoes a blue shift to 143.81–146.26 ppm in the complexes spectra. According to free ligand spectrum, the peak at 129.07 ppm was belonged to $C_{(1,1')}$ that is downfielded to 129.78–130.37 ppm in all complexes spectra. $C_{(4,4')}$ is assigned to a peak at 131.22 ppm in ligand spectrum that shifts to 134.76–135.36 ppm in the zinc complexes. Based on ligand spectrum, $C_{(2,2')}$ peak appeared in 128.72 ppm that is downfielded to the range of 128.97–129.11 ppm when the ligand is attached to the zinc ion. The signals appeared at 128.49, 127.47, 55.22 and 49.34 ppm are assigned to other ligand carbons of $C_{(3,3')}$, $C_{(6,6')}$, $C_{(8,8')}$ and $C_{(9,9')}$, respectively that all of them were upfielded to the ranges of 127.50–127.66, 125.12–127.45, 55.43–56.11 and 46.49–48.14 ppm at zinc complexes spectra. An additional signal with respect to other complexes, appeared at 134.04 ppm in zinc thiocyanate complex is assigned to $C_{(NCS)}$. Regarding the spectral data from ^{1}H and ^{13}C NMR spectra and a comparison between signal positions in ligand and zinc complexes well support the suggested structure for the zinc complexes (Scheme 1).

Crystal structure of zinc azide complex

Suitable crystal of 1 for X-ray structure analysis was grown from an ethanolic solution. The crystallographic and refinement data are tabulated as Table 3. Zinc azide complex crystallizes as triplet in trigonal system with space group of $P3_1$. There are three crystallographically independent (but chemically equivalent) molecules in the asymmetric unit. An ORTEP view of zinc azide complex is shown in Fig. 5. Selected bond parameters relevant to the Zn coordination sphere are collected in Table 4. The coordination sphere around the zinc centers is well described as five coordinated distorted trigonal bipyramide with three nitrogen atoms from Schiff base ligand and two terminal azide nitrogens bonded to zinc. The equatorial positions are occupied by the central nitrogen atom of the Schiff base ligand and two terminal azide nitrogen atoms while two azomethine nitrogen atoms of the Schiff base ligand occupy the axial positions. The axial bond angle (156.0(5)° in Zn1, 157.3(6)° in Zn2, and 157.0(5)° in Zn3 molecule) deviates from the ideal 180°, and this deviation is due to the structural constraints of the Schiff base ligand. The equatorial bond angles (115.0(6)–127.3(5)° in Zn1, 113.0(7)–129.7(7)° in Zn2, 111.4(6)–128.4(6)° in Zn3 molecule) also have some deviation from the ideal 120°. The sum of the three equatorial angles is 360° at Zn1, 359.9° at Zn2, and 359.9° at Zn3. The Zn—N_{imine} distances (axial bonds) are from 2.20(1) to 2.29(2) Å in the three molecules. The Zn—N_{amine} distance is 2.08(1) Å for Zn3 and 2.09(1) Å for Zn1 and Zn2. The Zn—N_{azide} bonds have the shortest length and range from 1.95(2) to 2.02(2) Å. All bond lengths and angles are within the range of other related complexes with similar geometry [44,45]. The dihedral angle between phenyl rings is 27.96° in Zn1, 40.84° in Zn2, and 32.45° in the Zn3 molecules.

Table 3
Crystal data and structure refinement for zinc azide complex.

Chemical formula	$C_{22}H_{25}N_9Zn$
Formula weight	480.88
Crystal system	Trigonal
Crystal size (mm)	0.50 × 0.25 × 0.20
Space group	$P3_1$
Temperature (°K)	293.0(2)
Wavelength (Å)	0.71073
a (Å)	28.104(2)
b (Å)	28.104(2)
c (Å)	7.9718(6)
α (°)	90
β (°)	90
γ (°)	120
V (Å^3)	5452.9(9)
Z	9
D_{calc} (Mg/m^3)	1.318
μ (mm^{-1})	1.041
$F(000)$	2250
Absorption correction	Semi-empirical from equivalents
Theta range for data collection (°)	3.348–25.348
Index ranges	$-29 \leqslant h \leqslant 33$ $-32 \leqslant k \leqslant 21$ $-9 \leqslant l \leqslant 9$
Maximum and minimum transmission	1.00000 and 0.27841
Refinement method	Full-matrix least-squares on F^2
Reflections collected	14560
Independent reflections	10322
R_{int}	0.0419
Goodness-of-fit (GOF) on F^2	1.090
Final R indices [$I > 2\sigma(I)$]	$R_1 = 0.0649$, $wR_2 = 0.1490$
R indices (all data)	$R_1 = 0.0844$, $wR_2 = 0.1734$
Data/restraints/parameters	10322/757/866
Largest difference in peak and hole (e Å^{-3})	0.519 and −0.588

The crystal lattice is packed by intermolecular interactions such as N—H···N, C—H···N and C—H…π hydrogen bonding interactions. Terminal azide groups participates in classic (N—H···N) and non-classic (C—H···N) hydrogen bonds. N—H···N hydrogen bonds are formed between N—H group of secondary amine of Schiff base ligand from one molecule and terminal azide nitrogen atoms from other molecule. There are three kinds of strong hydrogen bonds of N—H···N in the crystal structure (Table 3). Each independent molecule in asymmetric unit constitutes one of these bonds. Azide groups also involves in some C—H···N hydrogen bonds with aliphatic and aromatic hydrogen atoms of Schiff base ligand as donor (Table 5). Zn1, Zn2, and Zn3 molecules are connected to five, six, and four other molecule via X—H···N (X = C, N), respectively (Fig. 6). In addition, there are a number of C—H···π interactions in crystal structure of zinc azide complex that their distances and angles are well within the accepted rang of CH···π interactions (Table 5) [46]. These intermolecular interactions stabilize the molecular structure and lead to a three dimensional supramolecular structure.

Antibacterial bioassay (in vitro)

Antibacterial activities of the zinc complexes as compared with free ligand were tested by disk diffusion method. Two gram-positive (*S. aureus* and *B. subtilis*) and two gram-negative (*E. coli* and *P. aeruginosa*) bacteria were applied for these tests. The obtained data from biological evaluation have been tabulated as Table 6 in which diameter of

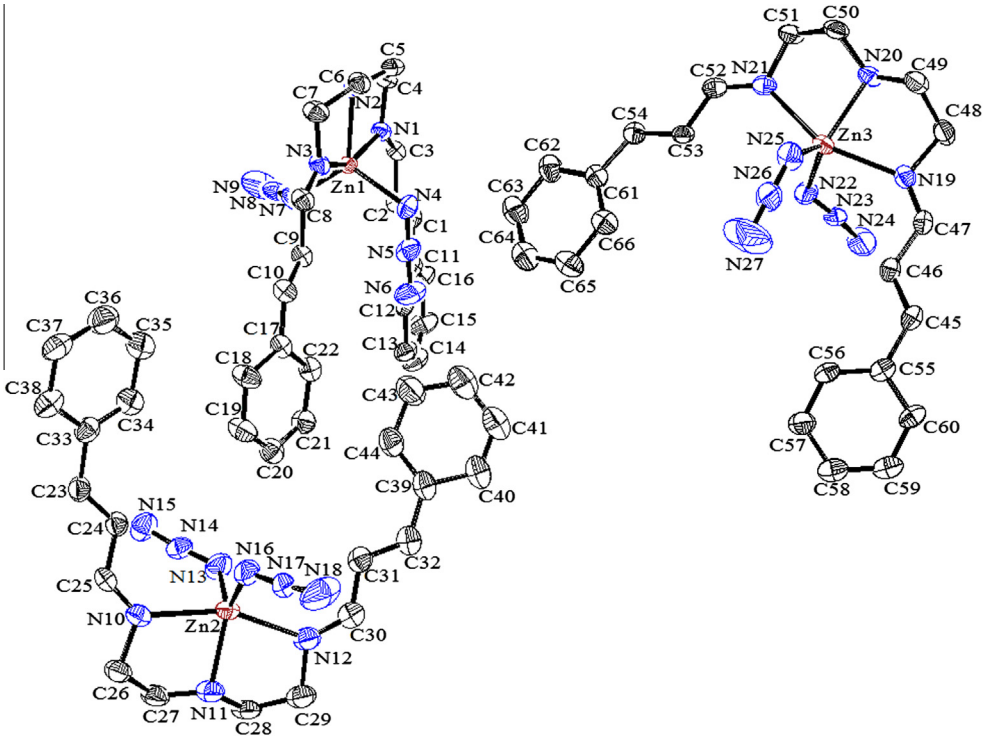

Fig. 5. ORTEP diagram of zinc azide complex with the atom numbering scheme. The atoms are represented by 20% probability thermal ellipsoids. Hydrogen atoms are omitted for clarity.

Table 4
Selected bond lengths (Å) and bond angles (°) data for zinc azide complex.

Molecule 1		Molecule 2		Molecule 3	
Bond length (Å)					
Zn1—N1	2.29(2)	Zn2—N10	2.25(1)	Zn3—N19	2.27(1)
Zn1—N2	2.09(1)	Zn2—N11	2.09(1)	Zn3—N20	2.08(1)
Zn1—N3	2.20(1)	Zn2—N12	2.23(1)	Zn3—N21	2.21(1)
Zn1—N4	1.99(1)	Zn2—N13	1.99(3)	Zn3—N22	1.98(2)
Zn1—N7	1.98(1)	Zn2—N16	1.95(2)	Zn3—N25	2.02(2)
N4—N5	1.18(2)	N13—N14	1.16(3)	N22—N23	1.14(2)
N5—N6	1.18(3)	N14—N15	1.14(3)	N23—N24	1.14(2)
N7—N8	1.12(3)	N16—N17	1.19(3)	N25—N26	1.14(3)
N8—N9	1.14(4)	N17—N18	1.14(4)	N26—N27	1.15(4)
Bond angle (°)					
N1—Zn1—N2	78.5(5)	N10—Zn2—N11	77.4(6)	N19—Zn3—N20	78.4(5)
N1—Zn1—N3	156.0(5)	N10—Zn2—N12	157.3(6)	N19—Zn3—N21	157.0(5)
N1—Zn1—N4	93.8(5)	N10—Zn2—N13	95.0(7)	N19—Zn3—N22	99.4(6)
N1—Zn1—N7	98.9(5)	N10—Zn2—N16	94.9(7)	N19—Zn3—N25	94.6(6)
N2—Zn1—N3	77.6(5)	N11—Zn2—N12	79.9(7)	N20—Zn3—N21	78.6(5)
N2—Zn1—N4	117.7(6)	N11—Zn2—N13	113.0(7)	N20—Zn3—N22	128.4(6)
N2—Zn1—N7	127.3(5)	N11—Zn2—N16	129.7(7)	N20—Zn3—N25	111.4(6)
N3—Zn1—N4	95.6(5)	N12—Zn2—N13	93.1(8)	N21—Zn3—N22	95.5(6)
N3—Zn1—N7	97.0(5)	N12—Zn2—N16	100.2(7)	N21—Zn3—N25	92.9(6)
N4—Zn1—N7	115.0(6)	N13—Zn2—N16	117.2(8)	N22—Zn3—N25	120.1(7)

inhibition zone from the growth (in mm) are reported as antibacterial activities. Based on the resultant data, the antibacterial tests of the zinc complexes (with disks soaked in 10, 20 and 30 mg/mL of active compound) showed different activity for them at the same conditions. In an overall view, it was found that the ligand has lower activity with respect to zinc complexes against microorganisms. According to Table 6, $ZnLI_2$ was found as the most effective compound against *B. subtilis*. The antibacterial activities of the zinc complexes against *S. aureus* can be ordered as following trend:

$$ZnL(N_3)_2 > ZnL(NCS)_2 > ZnLI_2 > ZnLBr_2 > ZnLCl_2 \sim \text{Ligand}$$

$ZnLCl_2$ and $ZnL(NCS)_2$ complexes were found to be the most impressive compounds against *P. aeruginosa* and *E. coli* respectively. Standard drugs including Amoxicillin, Penicillin and Cephalexin were used as positive blank to compare their antibacterial activities with the activities of the zinc complexes. Some images of inhibition zones around the constructed disks are shown in Fig. 7. All compounds showed acceptable efficiency against bacteria in comparison with standard compounds [30] so introducing these kinds of zinc complexes with bactericidal potential may be of interest in biochemistry point of view.

Table 5
Intermolecular interactions in zinc azide complex.

Interaction (D—H...A)		D—H (Å)	H···A (Å)	D···A (Å)	<A···H—D (°)
N—H···N	N2—H2N···N9^{i}	0.98(2)	2.06(4)	2.93(4)	147
	N11—H11N···N18^{ii}	0.98(2)	2.12(4)	2.99(4)	146
	N20—H20N···N24^{iii}	0.98(1)	2.09(2)	2.97(2)	148
C—H···N	C63—H63···N4	0.93(3)	2.53(2)	3.45(3)	173
	C62—H62···N6^{iv}	0.93(3)	2.71(2)	3.50(3)	143
	C4—H4A···N7^{v}	0.97(2)	2.67(1)	3.59(2)	160
	C5—H5B···N9^{iv}	0.97(2)	2.74(2)	3.68(3)	164
	C10—H10···N15^{iv}	0.93(2)	2.50(2)	3.41(3)	165
	C15—H15···N15^{v}	0.93(4)	2.55(2)	3.33(4)	142
	C35—H35···N15^{iv}	0.93(3)	2.60(2)	3.46(3)	153
	C27—H27A···N16^{vi}	0.97(2)	2.75(1)	3.65(2)	155
	C29—H29B···N16^{vii}	0.97(3)	2.70(2)	3.66(4)	170
	C26—H26B···N18^{viii}	0.97(3)	2.64(3)	3.35(3)	130
	C28—H28B···N18^{vi}	0.97(2)	2.69(4)	3.60(4)	156
	C48—H48B···N22^{ix}	0.97(3)	2.65(2)	3.57(4)	160
	C49—H49A···N24^{iv}	0.97(2)	2.74(2)	3.67(3)	161
	C37—H37···N27^{viii}	0.93(3)	2.48(3)	3.19(4)	134
C—H···π	C4—H4B···Cg(1)	0.97(2)	3.086	3.897	142
	C7—H7A···Cg(2)	0.97(2)	3.002	3.823	143
	C26—H26A···Cg(3)	0.97(2)	3.082	3.995	157
	C29—H29A···Cg(4)	0.97(2)	2.975	3.726	135
	C48—H48A···Cg(5)	0.97(3)	3.019	3.843	142
	C51—H51B···Cg(6)	0.97(3)	3.078	3.949	157

Symmetry transformations used to generate equivalent atoms: (i) $-y+1, x-y+1, z-2/3$, (ii) $-x+y-1, -x+1, z+2/3$, (iii) $-y+2, x-y+2, z-2/3$, (iv) $x, y, 1+z$, (v) $1-y, 1+x-y, z+1/3$, (vi) $x, y, -1+z$, (vii) $-1-x+y, 1-x, -1/3+z$, (viii) $1-y, 2+x-y, z-2/3$, (ix) $2-y, 2+x-y, 1/3+z$.
Ring code: Cg(1): C11, C12, C13, C14, C15, C16; Cg(2): C17, C18, C19, C20, C21, C22; Cg(3): C33, C34, C35, C36, C37, C38; Cg(4): C39, C40, C41, C42, C43, C44; Cg(5): C55, C56, C57, C58, C59, C60; Cg(6): C61, C62, C63, C64, C65, C66;

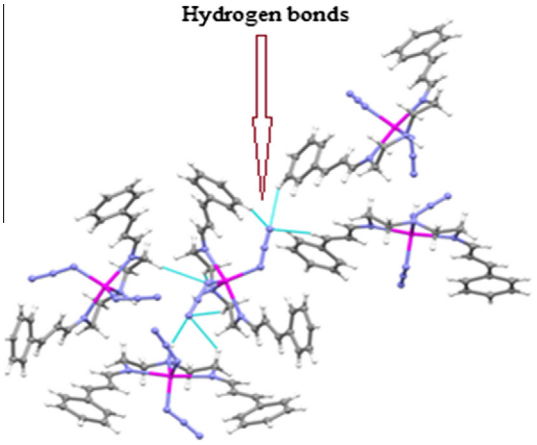

Fig. 6. Hydrogen bonds induced by azide groups in zinc azide complex structure.

Antifungal bioassay

All zinc complexes were screened for their *in vitro* antifungal activities against *C. albicans* and *A. niger* as two fungi by disk diffusion method [47]. The antifungal activities data as zone diameter of inhibition (mm) of the growth around the disk saturated with 10, 20 and 30 mg/mL of active compound have been compiled in Table 7. Similar to antibacterial activities, antifungal properties of the zinc complexes were found to be more notable as compared with free ligand. Among the complexes, $ZnLI_2$ showed more inhibitory effect against *C. albicans* whereas $ZnLCl_2$ was more impressive than other complexes against *A. niger*. Some properties such as structure and lipophilicity character of the tested compounds and cell membrane characteristics of microorganism may be considered as important factors controlling the antimicrobial activity. It seems that attaching the zinc cation to ligand causes suitable lipophilicity nature for the complexes facilitating their passage from microorganism cell wall [48]. This causes more effective block of the active site of enzyme of microorganisms which prevents their growth. Off course, the role of coordinated X ions with different electronegativity and steric effects may be effective on antimicrobial activities of the complexes [49].

Thermal analyses of the zinc complexes

Thermal analyses of the zinc complexes were performed under nitrogen atmosphere with the heating rates of 10 °C/min from room temperature to 1000 °C. Thermal stability of the zinc

Table 6
Antibacterial activity of the zinc complexes as diameter of zone of inhibition[a] (mm) around constructed disks (saturated with 10, 20 and/or 30 mg/mL) against some bacteria.

Compound	Gram-positive						Gram-negative					
	Bacillus subtilis			*Staphylococcus aureus*			*Pseudomonas aeruginosa*			*Escherichia coli*		
	10[b]	20	30	10	20	30	10	20	30	10	20	30
Ligand	10	12	12	11	12	13	8	10	11	R	R	6
$ZnLCl_2$	8	9	13	7	10	13	11	14	16	10	14	18
$ZnLBr_2$	10	13	15	9	10	14	9	10	14	9	12	18
$ZnLI_2$	25	27	30	10	14	17	11	11	11	12	14	20
$ZnL(NCS)_2$	10	11	13	13	16	18	8	9	11	19	20	21
$ZnL(N_3)_2$	22	23	23	15	17	19	12	13	15	16	17	20

[a] All data are the mean of two measurements.
[b] The numbers in this row refer to compound concentrations.

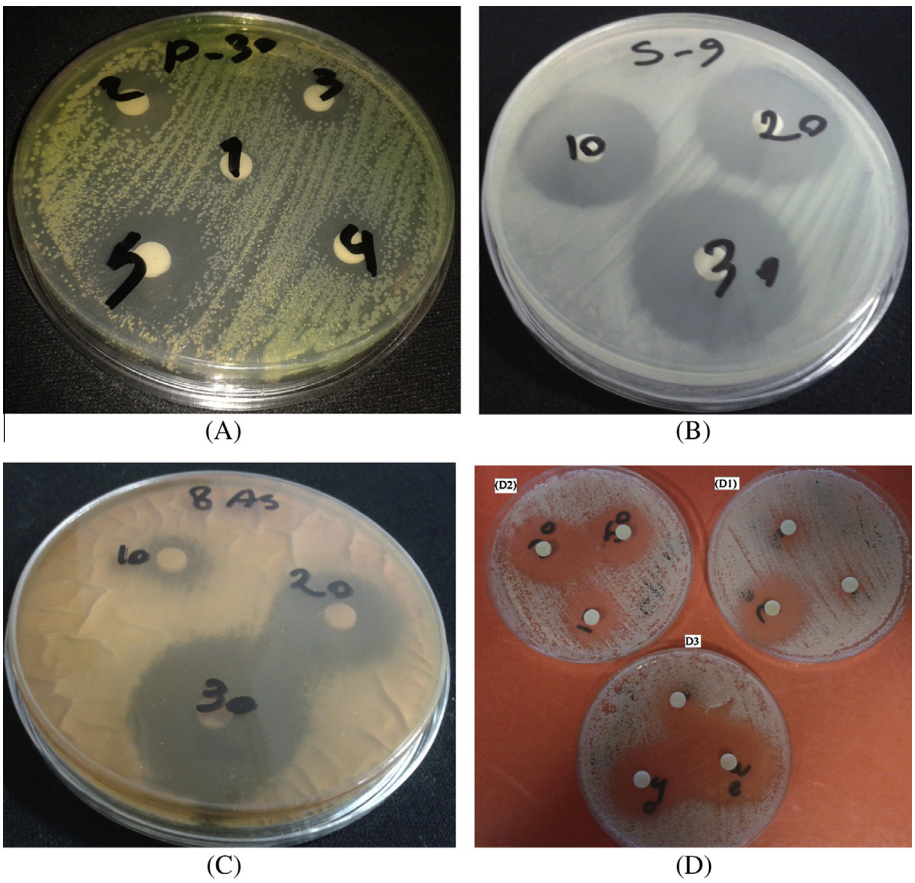

Fig. 7. Inhibition zone around the disks containing zinc complexes; (A) $ZnLI_2$ against *Pseudomonas aeruginosa*; (B) $ZnL(N_3)$ against *Staphylococcus aureus*; (C) $ZnL(NCS)_2$ against *Aspergillus niger*; (D) $ZnLCl_2$(D1), $ZnLBr_2$(D2) and $ZnLI_2$(D3).

Table 7
Antifungal activity of the compounds as diameter of zone of inhibition[a] (mm) around constructed disks (saturated with 10, 20 and/or 30 mg/mL) against two fungi.

Compound	*Candida albicans*			*Aspergillus niger*		
	10[b]	20	30	10	20	30
Ligand [33]	10	15	15	9	17	20
$ZnLCl_2$	7	22	27	10	33	40
$ZnLBr_2$	29	NR	NR	NR	22	32
$ZnLI_2$	15	26	34	R	24	35
$ZnL(NCS)_2$	20	24	30	15	18	20
$ZnL(N_3)_2$	21	22	23	17	17	18

[a] All data are the mean of two measurements.
[b] The numbers in this row refer to compound concentrations.

complexes and probable existence of water molecules inside or outside of the coordination sphere of them were two major reasons in this survey. The related thermal plots of complexes (TG/DTG/DTA) are depicted in Fig. 8. All thermo-gravimetric data including thermal decomposition ranges, mass loss (%) and kinetic activation parameters of each thermal decomposition step of the zinc complexes are collected in Table 8.

Since the TG plots shows no weight loss below the 200 °C, absence of water molecules in the complex structures is confirmed. According to thermal analyses data, it is found that the zinc complexes demonstrate different kinds of decomposition pathways. $ZnLCl_2$ is decomposed during four steps while $ZnLBr_2$ and $ZnLI_2$ are thermally destructed in three thermal steps. On the other hand, $ZnL(NCS)_2$ and $ZnL(N_3)_2$ exhibit different patterns so that two thermal steps are observed for decomposition process. Zinc halide complexes show two types of thermal behavior so that zinc iodide complex leave out a metallic residual of zinc but zinc chloride and bromide complexes are absolutely decomposed without any residual. Both of zinc azide and zinc thiocynate are decomposed with residuals of Zn(NCS) and Zn at the end respectively. It is found that in all zinc complexes, the organic segment including phenyl rings eliminated at first decomposition step. Among the complexes, $ZnLI_2$ had minimum mass loss in the first step with amount of 11.72% while the maximum mass loss in first step was belonged to $ZnL(NCS)_2$ with amount of 36.41%. Regarding Table 8, initial temperature for starting of decomposition for zinc complexes was in the range of 180–200 °C while final temperature was in the range of 530–750. Also, zinc halide complexes need higher temperature (700–750 °C) for entirely decomposition than zinc azide and zinc thiocynate (530–640), so zinc halide complexes, especially $ZnLCl_2$, were suggested to be more thermal stable against thermal decomposition. Furthermore, the thermodynamic activation parameters of decomposition processes of the complexes entitled as activation energy (ΔE^*), enthalpy (ΔH^*), entropy (ΔS^*) and Gibbs free energy change (ΔG^*) of the decomposition were estimated graphically by plotting of data based on the Coats–Redfern relation [50]. Table 9 summarizes the calculated data. The activation energies of thermal decomposition steps were evaluated in the range of 25.84–185.49 kJ/mol. The high values of the activation energies suggest thermal stability for the complexes. In all thermal steps, evaluated values for ΔS^* are negative. Negative values of ΔS^* nearly at all thermal steps indicate an ordered character or slower rate than normal processes for thermal decomposition steps [51]. Ultimately, ΔH^* and ΔG^* values have positive amount in the ranges of 20.28–185.49 and $(1.71–2.62) \times 10^2$ kJ/mol respectively representing endothermic pathway at all thermal steps.

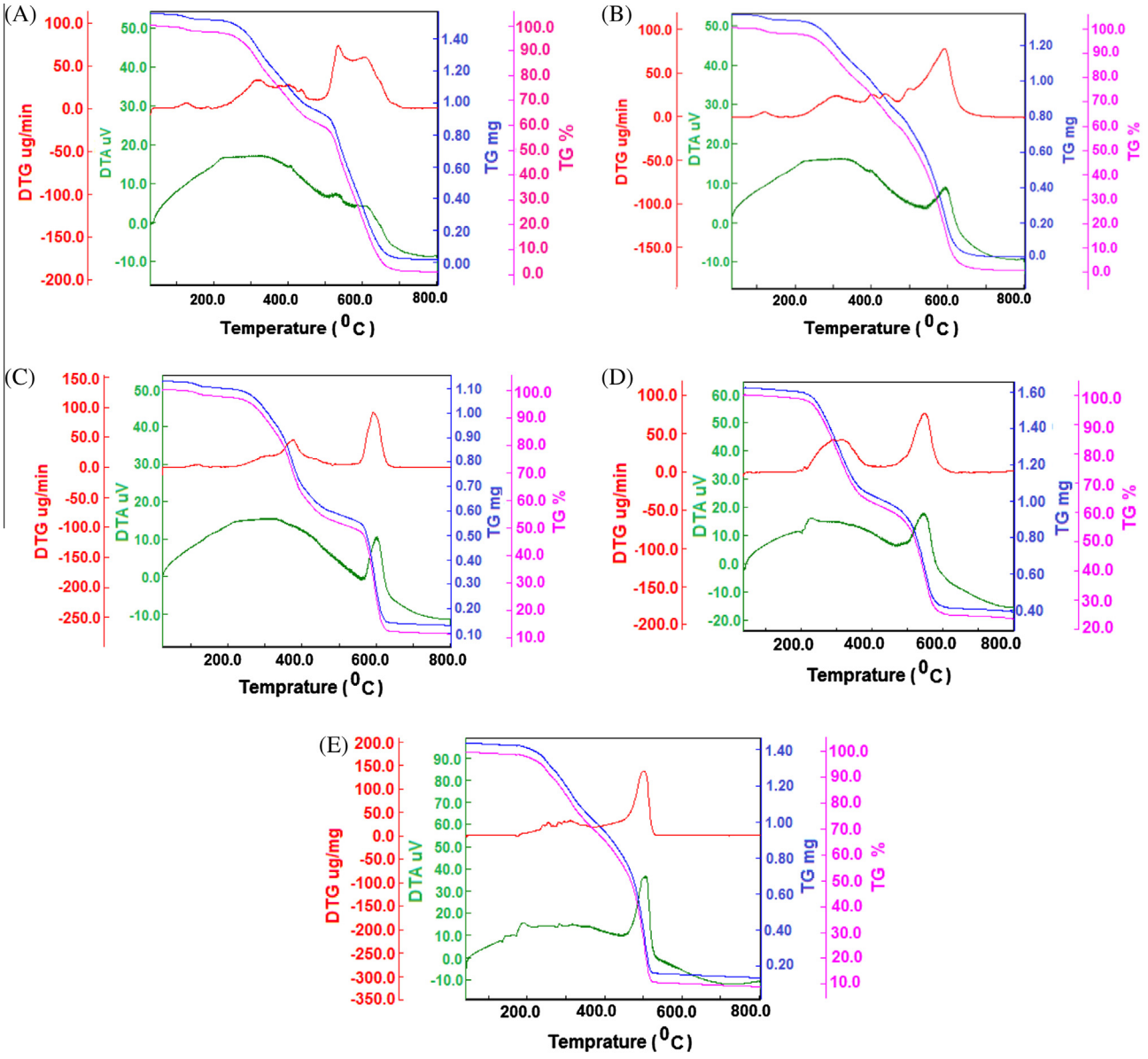

Fig. 8. TG/DTG/DTA plots of $ZnLCl_2$ (A), $ZnLBr_2$ (B), $ZnLI_2$ (C), $ZnL(NCS)_2$ (D) and $ZnL(N_3)_2$ (E) complexes.

Table 8
Thermal analysis data of the zinc complexes including temperature range, differential thermal gravimetry (DTG) peak, mass loss, proposed segment and final residuals.

Compound	Temperature range (°C)	Mass loss (%) found (Calculated)	DTG peak (°C)	Proposed segment	Final residue
$ZnLCl_2$	200–375	24.00 (24.17)	320	C_9H_8	–
	375–520	18.50 (18.75)	395	C_7H_6	
	520–585	29.22 (29.17)	530	$C_7H_{14}N_3$	
	585–750	27.02 (27.71)	605	$ZnCl_2$	
$ZnLBr_2$	180–370	20.43 (20.43)	305	C_9H_8	–
	370–474	20.49 (20.43)	415	C_9H_8	
	474–740	58.48 (59.14)	590	$C_5H_{12}N_3Br_2Zn$	
$ZnLI_2$	200–320	11.72 (11.60)	310	C_6H_5	Zn
	320–550	37.02 (40.62)	375	$C_{17}H_{23}N_3$	
	550–700	37.18 (38.22)	590	I_2	
$ZnL(NCS)_2$	200–425	36.41 (36.71)	305	$C_{15}H_{13}$	Zn(SCN)
	425–640	38.12 (37.20)	548	$C_9H_{15}N_4S$	
$ZnL(N3)_2$	200–360	26.36 (26.32)	310	C_9H_8N	Zn
	360–530	60.63 (60.75)	500	$C_{14}H_{20}N_8$	

Table 9
Thermo-kinetic parameters of the thermal decomposition steps of the zinc complexes.

Compound	Decomposition step (°C)	E^* (kJ/mol)	A^* (1/S)	ΔS^* (kJ/mol K)	ΔH^* (kJ/mol)	ΔG^* (kJ/mol)
$ZnLCl_2$	200–375	57.24	1.83×10^2	-2.07×10^2	52.31	1.75×10^2
	375–520	25.84	9.75×10^{-2}	-2.71×10^2	20.28	2.02×10^2
	520–585	96.11	2.89×10^3	-1.87×10^2	89.39	2.41×10^2
	585–750	78.31	8.62×10^1	-2.17×10^2	71.00	2.62×10^2
$ZnLBr_2$	180–370	37.14	2.53	-2.43×10^2	32.33	1.73×10^2
	370–474	43.65	3.19	-2.42×10^2	37.92	2.05×10^2
	474–630	55.33	4.03	-2.42×10^2	48.15	2.57×10^2
$ZnLI_2$	200–320	90.94	7.07×10^5	-1.38×10^2	86.15	1.66×10^2
	320–550	37.52	8.99×10^{-1}	-2.52×10^2	32.13	1.96×10^2
	550–700	104.92	4.75×10^3	-1.83×10^2	97.74	2.56×10^2
$ZnL(NCS)_2$	200–425	53.22	6.55×10^1	-2.16×10^2	48.33	1.75×10^2
	425–640	71.61	8.49×10^1	-2.16×10^2	64.77	2.43×10^2
$ZnL(N_3)_2$	200–360	53.80	1.38×10^2	-2.10×10^2	48.94	1.71×10^2
	360–530	191.93	5.83×10^{10}	-4.68×10^1	185.49	2.22×10^2

Conclusion

A series of some novel zinc complexes with a tridentate Schiff base ligand was successfully synthesized. In addition, the nano-structure forms of them have been also prepared under ultrasonic irradiation. The synthesized complexes were characterized by various spectral and physical methods such as FT-IR, UV–visible, ^{1}H and ^{13}C NMR, X-ray crystallography, thermal analyses, melting points and molar conductivity. Zinc azide complex structure was analyzed by X-ray crystallography. The complex crystallizes as a triplet in trigonal system with space group of $P3_1$. SEM, XRD and TEM techniques were used for investigation morphology and size of nano-structure complexes. Evaluation of antibacterial and antifungal activities of the zinc complexes with respect to free ligand was performed. Accordingly, $ZnLI_2$ and $ZnL(N_3)_2$ were found as the most effective agents among the zinc complexes against *B. subtilis* and *S. aureus* while $ZnLCl_2$ and $ZnL(NCS)_2$ showed good inhibitory effects against *P. aeruginosa* and *E. coli* respectively. Also among the complexes, $ZnLI_2$ and $ZnLCl_2$ were found as more impressive in fighting with *C. albicans* and *A. niger* with respect to others. Finally, thermal analyses of the zinc complexes revealed that they are decomposed via 2–4 thermal steps from room temperature to 1000 °C.

Acknowledgement

Partial support of this work by Yasouj University is appreciated. Also X-ray analysis by National University of Ireland is acknowledged.

References

[1] Y.-P. Ho, S.C.F. Au-Yeung, K.K.W. To, Med. Res. Rev. 23 (2003) 633–655.
[2] A.S. Abu-Surrah, M. Kettunen, Curr. Med. Chem. 13 (2006) 1337–1357.
[3] C.K. Murphy, E.G. Fey, B.A. Watkins, V. Wong, D. Rothstein, S.T. Sonis, Clin. Cancer Res. 14 (2008) 4292–4297.
[4] K.H. Thompson, J. Lichter, C. LeBel, M.C. Scaife, J.H. McNeill, C. Orvig, J. Inorg. Biochem. 103 (2009) 554–558.
[5] D. Dive, C. Biot, Chem. Med. Chem. 3 (2008) 383–391.
[6] F. Han, N. Shioda, S. Moriguchi, Z.-H. Qin, K. Fukunaga, Neuroscience 151 (2008) 671–679.
[7] L. Ronconi, P.J. Sadler, Coord. Chem. Rev. 251 (2007) 1633–1648.
[8] P.C.A. Bruijnincx, P.J. Sadler, Curr. Opin. Chem. Biol. 12 (2008) 197–206.
[9] B. Desoize, Anticancer Res. 24 (2004) 1529–1544.
[10] A.K.M. Nur Alam Siddiki, Md. Shahidur Rahman, Md. Arifur Rahman, Md. Abdus Salam, Md. Abu Yousuf, Md. Farhadul Islam, et al., Bangladesh Pharm. J. 15 (1) (2012) 83–87.
[11] M. Shebl, S.M.E. Khalil, S.A. Ahmed, H.A.A. Medien, J. Mol. Struct. 980 (2010) 39–50.
[12] S.K. Bharti, G. Nath, R. Tilak, S.K. Singh, Eur. J. Med. Chem. 45 (2010) 651–660.
[13] G. Kumar, V. Singh, K. Singh, I. Ahmad, D.S. Yadav, A. Kumar, N. Shishodia, J. Pharm. 2 (2012) 45.
[14] R.S. Hunoor, B.R. Patil, D.S. Badiger, R.S. Vadavi, K.B. Gudasi, V.M. Chandrashekhar, I.S. Muchchandi, Appl. Organomet. Chem. 25 (2011) 476–483.
[15] D. Kovala-Demertzi, D. Hadjipavlou-Litina, M. Staninska, A. Primikiri, C. Kotoglou, M.A. Demertzis, J. Enzyme Inhib. Med. Chem. 24 (2009) 742–752.
[16] N. Nishat, S. Hasnain, T. Ahmad, A. Parveen, J. Therm. Anal. Calorim. 105 (2011) 969–979.
[17] K.C. Gupta, A.K. Sutar, Coord. Chem. Rev. 252 (2008) 1420–1450.
[18] P.G. Cozzi, Chem. Soc. Rev. 33 (2004) 410–421.
[19] H.F. Abd El-Halim, F.A. Nour El-Dien, G.G. Mohamed, N.A. Mohamed, J. Therm. Anal. Calorim. 109 (2012) 883–892.
[20] A. Jarrahpour, D. Khalili, E. De Clercq, C. Salmi, J.M. Brunel, Molecules 12 (2007) 1720–1730.
[21] G.H. Clever, M. Shionoya, Coord. Chem. Rev. 254 (2010) 2391–2402.
[22] D.D. Qin, Z.Y. Yang, F.H. Zhang, B. Du, P. Wang, T.R. Li, Inorg. Chem. Commun. 13 (2010) 727–729.
[23] N. Shahabadi, S. Kashanian, F. Darabi, Eur. J. Med. Chem. 45 (2010) 4239–4245.
[24] F. Kim, S. Connor, H. Song, T. Kuykendall, P.D. Yang, Angew. Chem. Int. Ed. 43 (2004) 3673.
[25] H. Zhang, D.R. Yang, D.S. Li, X.Y. Ma, S.Z. Li, D.L. Que, Cryst. Growth Des. 5 (2005) 547.
[26] M.H. Habibi, E. Askari, M. Habibi, M. Zendehdel, Spectrochim. Acta A 104 (2013) 197.
[27] M.H. Habibi, M.H. Rahmati, Spectrochim. Acta A 133 (2014) 13.
[28] M. Montazerozohori, S.A.R. Musavi, J. Coord. Chem. 61 (2008) 3934–3942.
[29] M. Montazerozohori, S. Yadegari, A. Naghiha, S. Veyseh, J. Ind. Eng. Chem. 20 (2014) 118.
[30] M. Montazerozohori, S. Zahedi, A. Naghiha, M. Montazer Zohour, Mater. Sci. Eng. C 35 (2014) 195.
[31] M. Montazerozohori, S.A. Musavi, A. Naghiha, M. Montazer Zohour, Spectrochim. Acta A 129 (2014) 382.
[32] M. Montazerozohori, S.A. Musavi, A. Naghiha, S. Veyseh, J. Chem. Sci. 126 (2014) 227.
[33] M. Montazerozohori, S. Mojahedi Jahromi, A. Naghiha, J. Ind. Eng. Chem. (2014), http://dx.doi.org/10.1016/j.jiec.2014.07.017.
[34] G. Sheldrick, Acta Cryst. Section A 64 (1) (2008) 112–122.
[35] P. McArdle, K. Gilligan, D. Cunningham, R. Dark, M. Mahon, Cryst. Eng. Comm. 6 (53) (2004) 303–309.
[36] A.W. Bauer, W.M. Kirby, J.C. Sherris, M. Turck, Am. J. Clin. Pathol. 45 (1966) 493–496.
[37] Atta-ur-Rahman, M.I. Choudhary, W.J. Thomsen, Bioassay Techniques for Drug Development, Harwood Academic Publishers, Amsterdam, The Netherlands, 2001. pp. 22.
[38] M. Sonmez, A. Levent, M. Sekerci, Synth. React. Inorg. Met. Org. Chem. 33 (10) (2003) 1747–1761.
[39] N. Dharmaraj, P. Viswanathamurthi, K. Natarajan, Trans. Met. Chem. 26 (2001) 105–109.
[40] B. Samanta, J. Chakraborty, C.R. Choudhury, S.K. Dey, D.K. Dey, S.R. Batten, P. Jensen, G.P.A. Yap, S. Mitra, Struct. Chem. 18 (2007) 33–41.
[41] M. Montazerozohori, S.A. Musavi, A. Masoudiasl, A. Naghiha, M. Dusek, M. Kucerakova, Spectrochim. Acta A 137 (2015) 389–396.
[42] Z.H. Chohan, Trans. Met. Chem. 34 (2009) 153–161.
[43] K. Singh, M.S. Barwa, P. Tyagi, Eur. J. Med. Chem. 41 (2006) 147–153.
[44] R. Ghosh, S.H. Rahaman, Ch.-N. Lin, T.-H. Lu, B.K. Ghosh, Polyhedron 25 (2006) 3104.
[45] H.C. Fang, Y.-Y. Ge, H.-Y. Jia, Sh.-S.h. Li, F. Sun, L.-G. Zhang, Y.-P. Cai, CrystEngComm 13 (2011) 67.
[46] M. Nishio, M. Hirota, Y. Umezawa, in: A.P. Marchand (Ed.), Methods in Stereochemical Analysis, Wiley-VCH, New York, 1998. pp. 19 and 33.

[47] NCCLS Reference Method for Broth Dilution Antifungal Susceptibility Testing of Yeasts; Proposed Standard NCCLS document M27-P, National Committee for Clinical Laboratory Standards, Wayne, 1992.
[48] B.G. Tweedy, Phytopathology 55 (1964) 910–914.
[49] V. Zelenak, K. Gyoryova, D. Mlynarcik, Met. Based Drugs 8 (2002) 269–274.
[50] A.W. Coats, J.P. Redfern, Nature 201 (1964) 68–69.
[51] N. Sharma, A.M. Thakur, S.S. Bhatt, S.C. Chaudhry, J. Chem. Sci. 119 (2007) 311.